Hindawi
International Journal of Photoenergy
Volume 2019, Article ID 4360816, 7 pages
https://doi.org/10.1155/2019/4360816

Research Article

Surface Treatment on Nickel Oxide to Enhance the Efficiency of Inverted Perovskite Solar Cells

Kaijie Wang,[1] Ye Tian,[2] Heng Jiang,[3] Meng Chen,[3] and Shuangyan Xu[4]

[1]*Beijing Tongren Eye Center, Beijing Tongren Hospital, Capital Medical University, Beijing Ophthalmology & Visual Sciences Key Lab, Beijing, China*
[2]*Xi'an Simu Intelligent Technology Co. Ltd., Xi'an 710000, China*
[3]*Key Laboratory of Microgravity, Institute of Mechanics, Chinese Academy of Sciences, Beijing 100190, China*
[4]*School of Aeronautics, Northwestern Polytechnical University, Xi'an 710072, China*

Correspondence should be addressed to Ye Tian; ty@matheam.com and Shuangyan Xu; xushyan@nwpu.edu.cn

Received 8 July 2019; Revised 15 August 2019; Accepted 6 September 2019; Published 4 November 2019

Guest Editor: Yuanhang Cheng

The organic-inorganic hybrid perovskites such as $CH_3NH_3PbI_3$ have been considered as one of the most promising candidates for the next-generation photovoltaic materials due to its high absorption coefficient, low exciton binding energy, and long diffusion length. Herein, we have chosen NiOx as the hole transport material because metal oxides exhibit robust properties in air. We synthesized the NiOx film by a common sol-gel method. It is found that high-temperature annealing (500°C) is required to ensure the perovskite solar cell (PSC) with an efficiency over 15%. Low-temperature annealing (100°C) cannot convert the precursor materials to fully covered NiOx film, while the PSC based on mediate-temperature annealing (300°C) NiOx has larger resistance and thus lower efficiency. Fortunately, we have found that UV-ozone treatment on the NiOx film can reduce the resistance of the device based on 300°C annealed NiOx. The champion device can reach 16% efficiency with UV-ozone-treated 300°C annealed NiOx. This work has made it possible to reduce the annealing temperature of the sol-gel NiOx for high-efficiency PSCs, and it is believed that this simple surface treatment can be further employed in other metal oxide-based optoelectronic devices.

1. Introduction

The organic-inorganic hybrid perovskite solar cells (PSCs) have made impressive progress after the first demonstration of 3.8% power conversion efficiency (PCE) with a dye-sensitized solar cell architecture in 2009 [1]. The impressive optoelectronic properties, such as high light absorption coefficient [2], low exciton binding energy, and long charge carrier diffusion length [3], have attracted researchers in the whole world to develop the PSCs. Thanks to the introduction of the solid film structure in the PSCs by Park et al. and Snaith et al., the record PCE of the PSCs has increased significantly to 24.2% in 2019 [4–6]. The solid state PSCs can be divided into two groups which are mesoporous structure and planar structure. The mesoporous structure requires a complicated process and high-temperature annealing to form the porous structure, while the planar structure is relatively simple and thus attracts much attention in the field [7–9].

Generally, the planar PSCs have either normal n-i-p structure with the electron transport layer on the bottom electrode or inverted structure with the hole transport layer on the bottom electrode [10]. In this study, we fabricated the PSCs based on the inverted structure. For this structure, there are several reports using organic semiconductors such as PEDOT:PSS [11], Poly-TPD [12], P3HT [13], and PTAA [14] to push the device efficiency over 16%. However, the degradation of the organic materials in ambient air makes the PSCs exhibit a poor stability. Therefore, researchers tried to employ robust inorganic semiconductors, mainly metal oxide such as ZnO and NiOx, as the charge-transporting materials to improve the device stability. There are already many reports on inverted PSCs based on NiOx. For example, Islam et al. fabricated NiOx by the sputtering method and the

PSCs based on the sputtered NiOx show higher PCE and stability than the PSCs based on PEDOT:PSS [15]. Abzieher et al. have demonstrated that electron beam-evaporated NiOx also exhibits higher performance for PSCs with 18.5% PCE [16]. These two methods are vacuum-related process which requires the specific equipment. On the other hand, solution-processed NiOx is relatively simple and can be available for a researcher in the field. You et al. have reported that a PSC with a p-i-n structure (glass/indium tin oxide/-NiOx/perovskite/ZnO/Al) fabricated by solution process exhibits 16.1% efficiency and high stability in air because the metal oxides prevent the perovskite from degradation in air [17]. He et al. have reported a new solution method to fabricate the ligand-free NiOx for PSCs and pushed the device efficiency to 18.49% [18]. Furthermore, Li et al. have applied graphene oxide (GO) to incorporate into the NiOx film to further improve its conductivity and they made a PSC with high fill factor over 80% and PCE over 19% [19]. Interface engineering is another approach to enhance the PCE of the PSCs. Cheng et al. have recently reported a light-soaking effect in NiOx-based PSCs due to the surface dipole on the NiOx film. They introduced an interface modification with organic small molecules to eliminate the light-soaking effect and push the PCE over 18% [20]. Surface modification on the NiOx nanoparticles has been also demonstrated to be an efficient way to improve the crystallization process of perovskite and the corresponding device efficiency [21].

Here in this work, we employed a common sol-gel method to prepare NiOx precursor films on cleaned FTO glasses. Firstly, we found that the annealing temperature is critical to form a uniform NiOx layer. From the film morphologies obtained by a Scanning Electron Microscope (SEM), it is obvious that low-temperature annealing (100°C) is not sufficient to form a fully covered NiOx on FTO, and thus, the perovskite film on it has a large amount of pinholes. The morphologies of perovskite films on NiOx films with 300°C and 500°C annealing do not exhibit obvious difference. However, the corresponding PSCs have different JV characteristics. The PSCs based on 500°C annealed NiOx have definitely higher photovoltaic parameters, and the PCE of the device can reach 15.3%. Our results demonstrated that the PSC based on 300°C annealed NiOx has higher series resistance. Inspired by the previous reports that doping NiOx by other elements can improve its conductivity, we thereby applied a simple UV-ozone treatment on the 300°C annealed NiOx and it is found that the series resistance of the PSC has been reduced and the champion PCE of this device has reached over 16%. Although there is only a little improvement compared to the PSC based on 500°C annealed NiOx, the advantage of our method is the annealing temperature of the sol-gel NiOx can be reduced to 300°C. It is believed that this method can be used on other solution-processed metal oxides not only for solar cells but also for other optoelectronic devices.

2. Materials and Methods

2.1. Materials. The precursor materials for NiOx sol-gel solution such as nickel acetate tetrahydrate, monoethanolamine, and anhydrous ethanol were purchased from Sinopharm Chemical Reagent Co. Ltd. Lead iodide (PbI_2), methylammonium iodide (MAI), phenyl-C61-butyric acid methyl ester ($PC_{61}BM$), and bathocuproine (BCP) for PSCs were bought from Xi'an Polymer Light Technology Corp. Anhydrous N,N-dimethylformamide (DMF), dimethyl sulfoxide (DMSO), chlorobenzene (CB), and toluene were purchased from Sigma-Aldrich.

2.2. NiOx Film Fabrication. The NiOx sol-gel precursor was prepared by dissolving the nickel acetate tetrahydrate and monoethanolamine in anhydrous ethanol at 60°C for half an hour according to previous report [22]. Then, 200 μL precursor solution was dropped on the cleaned FTO glass and spin-coated at 4000 rpm for 40 s. Finally, the NiOx films were annealed at 100°C, 300°C, and 500°C in ambient air for 1 hour to form the NiOx layer. For the UV-ozone treatment, the 300°C annealed NiOx film was put inside a UV-ozone cleaner (144A-220, Jelight Co. Inc.) and treated for 15 minutes.

2.3. Perovskite Solar Cell Fabrication. To prepare the perovskite precursor solution, PbI_2, MAI, and DMSO with 1 : 1 : 1 mole ratio were dissolved in DMF. Then, the perovskite films were fabricated by a one-step spin coating process [23]. For details, the perovskite precursor solution was dropped on the top of the NiOx films and then spun at 4000 rpm for 40 s. During the spinning, 200 μL toluene was dropped on the middle of the film. Then, the perovskite films were annealed at 100°C for 10 min in a N_2-filled glovebox. Then, the $PC_{61}BM$ layer was deposited on the top of perovskite by spin coating its solution (25 mg/mL in CB) at 2000 rpm for 40 s. Then, the BCP (1 mg/mL in ethanol) layer was coated on the top with 2000 rpm for 40 s. Finally, the Ag electrode was deposited on the top with thermal evaporation. The active area of the solar cell is 0.06 cm^2.

2.4. Characterizations. The top view morphologies of the NiOx layers and perovskite films were obtained by Scanning Electron Microscopy (SEM, Carl Zeiss). The UV-vis absorption of the films was conducted on a LAMBDA750 UV/vis/NIR spectrophotometer. The X-ray diffraction (XRD) pattern of perovskite films was performed on an X'Pert PRO instrument using Cu Kα ($\lambda = 0.154$ nm) radiation. The steady-state photoluminescence (PL) spectra of the perovskite films on different substrates have been measured with the excitation of 520 nm. The JV characteristics of different PSCs were measured under standard 1 sun AM 1.5 G illumination. The external quantum efficiency (EQE) profiles of the PSCs were measured by the Newport Oriel IQE-200 system without any voltage bias and light bias. The transient photocurrent curves were obtained on a digital oscilloscope connected to the devices and a 50 Ω resistor.

3. Results and Discussion

The planar p-i-n device structure studied in this paper has been illustrated in Figure 1(a). As can be seen, the $CH_3NH_3PbI_3$ perovskite film was sandwiched between the NiOx layer and the $PC_{61}BM$ layer. The BCP on the top of $PC_{61}BM$ is used to block the transport of holes. As shown

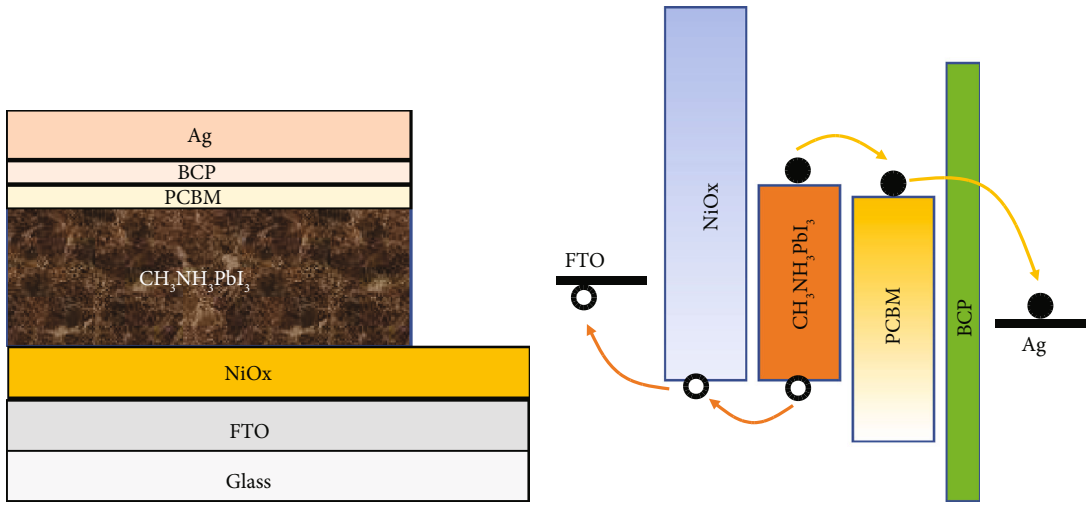

(a) (b)

Figure 1: (a) Schematic illustration of the planar PSC architecture; (b) the band alignment and charge carrier transport in the planar PSC.

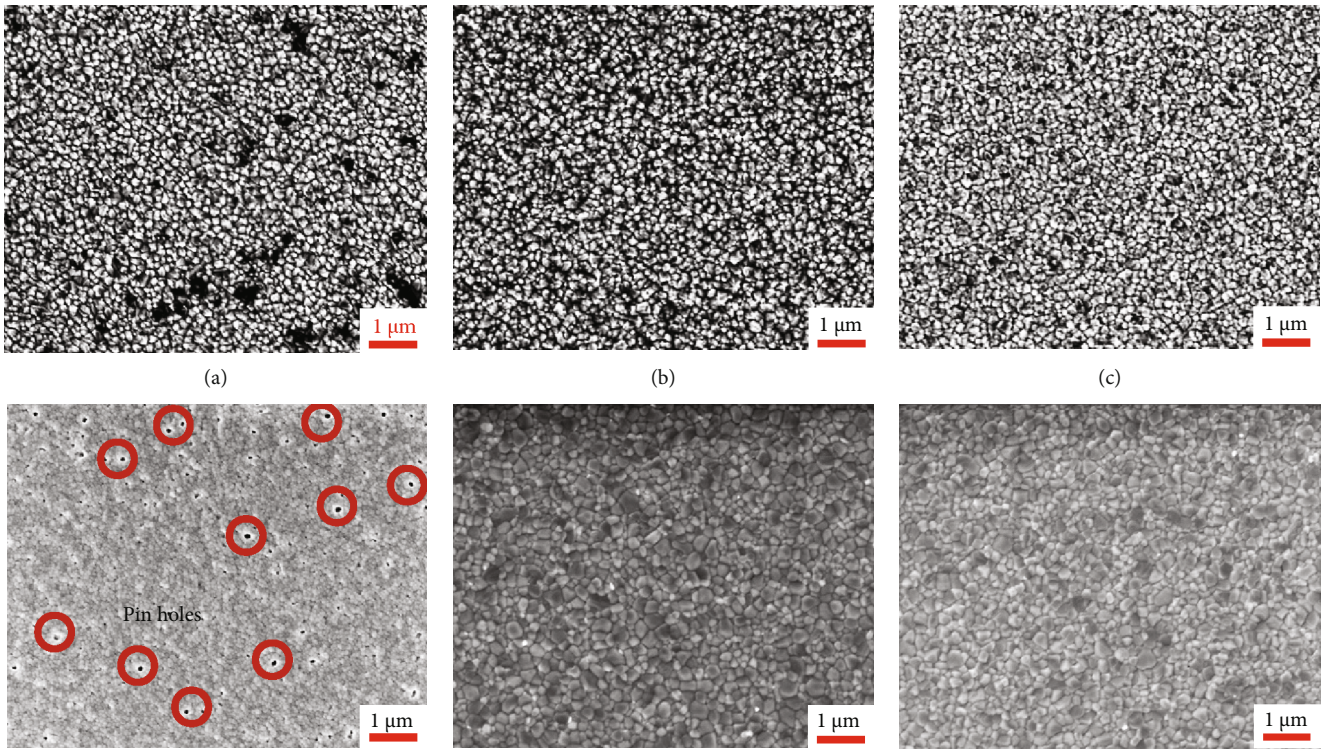

(a) (b) (c)

(d) (e) (f)

Figure 2: The top view morphologies of (a) NiOx annealed at 100°C, (b) NiOx annealed at 300°C, and (c) NiOx at 500°C. The top view morphologies of perovskite films deposited on (d) NiOx annealed at 100°C, (e) NiOx annealed at 300°C, and (f) NiOx at 500°C.

in Figure 1(b), the perovskite film absorbs the light under illumination and generates holes and electrons [24]. The holes will transport from NiOx to FTO electrode, while the electrons will transport through the $PC_{61}BM$ and BCP to the Ag electrode.

In order to investigate the effect of NiOx annealing temperature on the crystallization of perovskite films and thus the device photovoltaic performance, we firstly conducted the SEM to study the morphologies of NiOx films with different annealing temperatures. As shown in Figure 2(a), the NiOx film annealed at 100°C has not fully covered the FTO substrate. There are large amounts of pinholes in the film. On the other hand, the NiOx films annealed at 300°C and 500°C exhibit similar morphologies and no pinholes in the films, as can be seen in Figures 2(b) and 2(c).

We further measured the morphologies of perovskite films deposited on these three NiOx films. Figure 2(d) shows the perovskite morphology on the NiOx annealed at 100°C. It

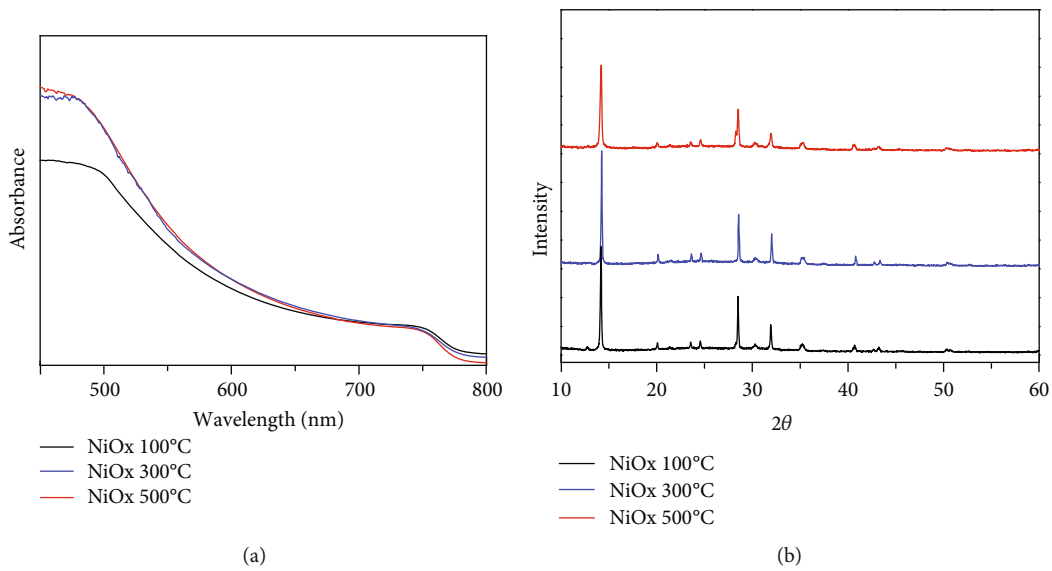

Figure 3: The UV absorption profiles (a) and XRD patterns (b) of perovskite films deposited on NiOx annealed at 100°C, 300°C, and 500°C.

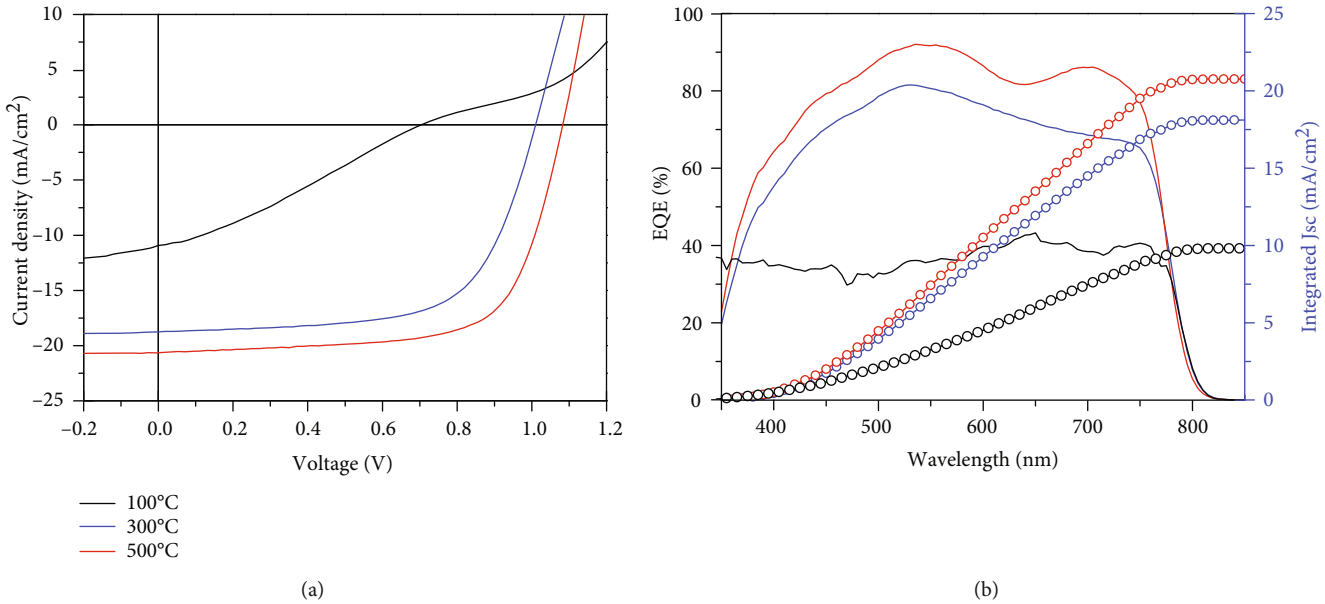

Figure 4: (a) The JV curves and (b) EQE profiles of perovskite solar cells based on NiOx annealed at 100°C, 300°C, and 500°C.

is obvious that there are pinholes in the film as labelled with red circles in the figure. On the contrary, the perovskite films on the NiOx annealed at 300°C and 500°C have the same morphology and they are compact without any pinholes. Therefore, it can be concluded that 100°C is not sufficient to obtain a fully covered NiOx film, while 300°C and 500°C annealing NiOx films have the same effect on perovskite film formation.

Figure 3(a) shows the UV-vis absorption profiles of perovskite films on NiOx annealed at 100°C, 300°C, and 500°C, which obviously demonstrate that the perovskite can be formed on NiOx regardless of the annealing temperature. However, the perovskite films on 100°C annealed NiOx have the lowest absorption, while the absorption of perovskite films on 300°C and 500°C annealed NiOx is the same. In order to further confirm the effect of NiOx annealing temperature on the crystallization of perovskite films, the XRD patterns of perovskite films have been measured and shown in Figure 3(b). There is no difference among these three films. Therefore, the NiOx annealing temperature has negligible effect on the crystallization of perovskite films.

The JV curves of PSCs based on NiOx films annealed at different temperature were shown in Figure 4(a), and the corresponding photovoltaic parameters are listed in Table 1. It is obvious that the PSC based on 500°C annealed NiOx exhibits the highest PCE of 15.5% with a Voc of 1.08 V, a Jsc of 20.7 mA/cm^2, and a FF of 69%. The PSC fabricated with 300°C annealed NiOx has a similar JV characteristic with a

Table 1: The photovoltaic performance of PSCs based on NiOx films annealed at different temperatures.

NiOx annealing temperature (°C)	Voc (V)	Jsc (mA/cm^2)	FF (%)	PCE (%)	Rs (Ω cm^2)	Rsh (Ω cm^2)
100	0.70	10.9	29	2.3	58.2	100.1
300	1.02	18.8	64	12.3	7.1	1102.7
500	1.08	20.7	69	15.3	6.0	1211.0
UV-ozone (300)	1.08	20.3	74	16.2	5.9	1359.3

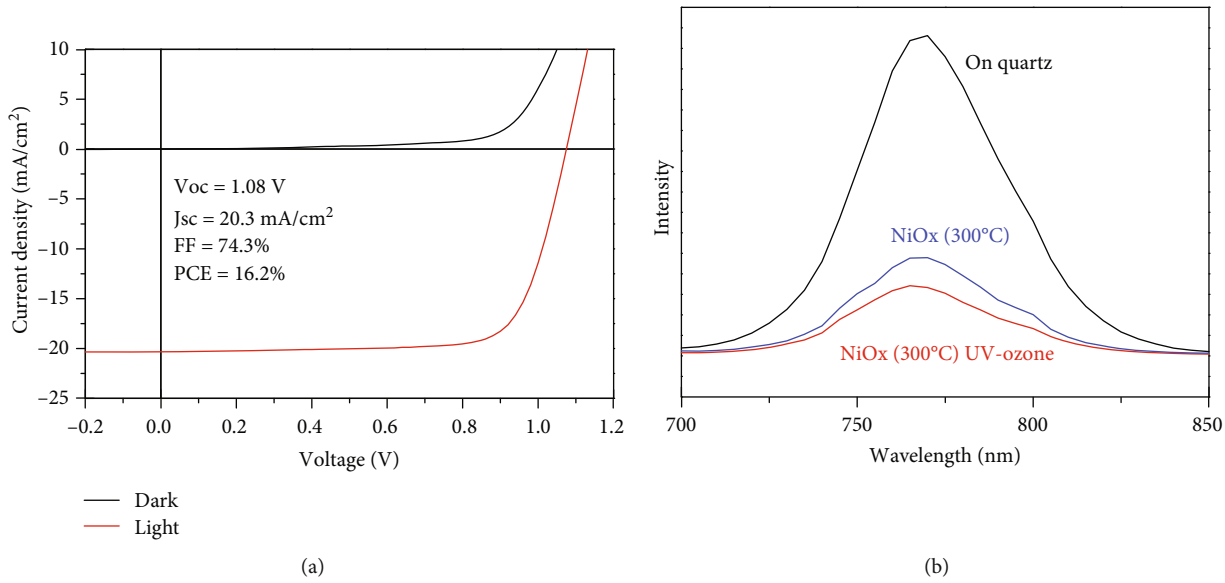

Figure 5: (a) The *JV* curve of the perovskite solar cell based on 300°C annealed NiOx with UV-ozone treatment. (b) The PL profiles of perovskite films deposited on quartz, 300°C annealed NiOx with and without UV-ozone.

Voc of 1.02 V, a Jsc of 18.8 mA/cm2, a FF of 64%, and a PCE of 12.3%. As shown in Table 1, the worse device performance is due to the higher series resistance and smaller shunt resistance. Therefore, the NiOx annealed at 300°C has worse conductivity than that annealed at 500°C. The PSC based on the 100°C annealed NiOx shows an "S-shape" in the *JV* curve as reported before, which is believed to be due to the unbalanced charge carrier extraction in the device [25].

Inspired by the previous reports that doping the NiOx films with other elements can further increase the conductivity of the NiOx films [26, 27], we then employed a simple UV-ozone to treat the 300°C annealed NiOx films, which is expected to dope the NiOx films with oxygen [28, 29]. The PSC based on the UV-ozone-treated NiOx is presented in Figure 5(a). As can be seen, the FF of the device has been increased from 69% to 74% after UV-ozone treatment on the NiOx film annealed at 300°C. As expected, the series resistance of this device has reduced to 5.9 Ω cm^2 which is even lower than that of NiOx annealed at 500°C. The details of the photovoltaic parameters are listed in Table 1. Our finding is consistent with the most recently reported work that UV-ozone can improve the performance of PSC based on NiOx films. The difference of our work is that we have found that UV-ozone can reduce the NiOx annealing temperature from 500°C to 300°C. We further performed PL measurement to study the charge carrier extraction behaviour of perovskite films deposited on 300°C annealed NiOx with and without UV-ozone treatment. The corresponding results can be seen in Figure 5(b). As can be seen, the perovskite film deposited on quartz has the strongest intensity. On the other hand, the perovskite deposited on the UV-ozone-treated NiOx has the lowest intensity, indicating that the hole extraction in the UV-ozone-treated NiOx is the most efficient [30, 31]. The results are consistent with the *JV* performance of the device. We further conducted transient photocurrent measurements on the PSCs based on 300°C annealed NiOx and UV-ozone-treated 300°C annealed NiOx. The results are shown in Figure 6. It is obvious that the current decay is faster in UV-ozone-treated 300°C annealed NiOx than that in the PSC based on 300°C annealed NiOx, indicating that the charge carrier transport is faster in the UV-ozone-treated device, which is in good agreement with PL results.

4. Conclusions

To conclude, we have employed a sol-gel method to fabricate the NiOx film for perovskite solar cells. It is found that the 100°C annealing is not sufficient to form a fully covered NiOx film on FTO glass. The 300°C and 500°C annealing exhibit similar NiOx morphology without pinholes. We further found that the perovskite films have the same crystallization and morphology on NiOx films annealed at 300°C and 500°C. The device performance indicates that the 300°C annealing NiOx has a bit higher resistance than the

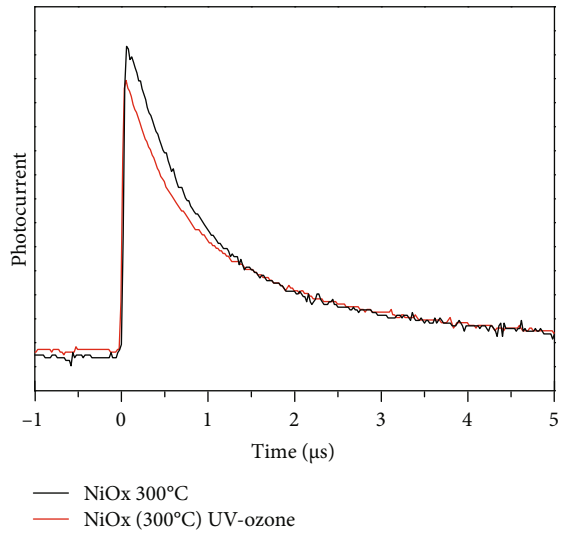

Figure 6: The transient photocurrent curves of the perovskite solar cell based on 300°C annealed NiOx with and without UV-ozone treatment.

500°C annealed NiOx. Finally, we applied UV-ozone to treat the 300°C annealed NiOx and found that the conductivity has increased after UV-ozone. The device performance also exhibits enhancement from 12% to 16% after UV-ozone treatment. Our results demonstrate that the UV-ozone method may be a promising approach to enhance the device performance not only for solar cells but also for other optoelectronic devices based on metal oxides.

Data Availability

The data used to support the findings of this study are available from the corresponding authors upon request.

Conflicts of Interest

The authors declare that there is no conflict of interest regarding the publication of this paper.

Acknowledgments

This study was supported by the Beijing Nova Program (Z151100000315096), the Beijing Municipal Science & Technology Commission (Z191100002019013), the Beijing Natural Science Foundation (7172056), and the priming scientific research foundation for the senior researchers in Beijing Tongren Hospital, Capital Medical University (2016-YJJ-GGL-010).

References

[1] A. Kojima, K. Teshima, Y. Shirai, and T. Miyasaka, "Organometal halide perovskites as visible-light sensitizers for photovoltaic cells," *Journal of the American Chemical Society*, vol. 131, no. 17, pp. 6050-6051, 2009.

[2] S. Yuan, Y. Cai, S. Yang et al., "Simultaneous cesium and acetate coalloying improves efficiency and stability of $FA_{0.85}MA_{0.15}PbI_3$ perovskite solar cell with an efficiency of 21.95%," *Solar RRL*, vol. 3, no. 9, article 1900220, 2019.

[3] G. Xing, N. Mathews, S. Sun et al., "Long-range balanced electron- and hole-transport lengths in organic-inorganic $CH_3NH_3PbI_3$," *Science*, vol. 342, no. 6156, pp. 344–347, 2013.

[4] H.-S. Kim, C. R. Lee, J. H. Im et al., "Lead iodide perovskite sensitized all-solid-state submicron thin film mesoscopic solar cell with efficiency exceeding 9%," *Scientific Reports*, vol. 2, no. 1, p. 591, 2012.

[5] M. M. Lee, J. Teuscher, T. Miyasaka, T. N. Murakami, and H. J. Snaith, "Efficient hybrid solar cells based on meso-superstructured organometal halide perovskites," *Science*, vol. 338, no. 6107, pp. 643–647, 2012.

[6] Y. Cheng, F. So, and S.-W. Tsang, "Progress in air-processed perovskite solar cells: from crystallization to photovoltaic performance," *Materials Horizons*, vol. 6, no. 8, pp. 1611–1624, 2019.

[7] A. K. Ravuvari, S. Yechuri, C. Chaitanya, and C. Rajesh, "Improved light efficiency in Si solar cells by coating mesoporous TiO_2 and cu-modified mesoporous TiO_2," *Solar RRL*, vol. 2, no. 12, article 1800214, 2018.

[8] L. Hu, J. Fu, K. Yang et al., "Inhibition of in-plane charge transport in hole transfer layer to achieve high fill factor for inverted planar perovskite solar cells," *Solar RRL*, vol. 3, no. 7, article 1900104, 2019.

[9] Z. Li, T. R. Klein, D. H. Kim et al., "Scalable fabrication of perovskite solar cells," *Nature Reviews Materials*, vol. 3, no. 4, article 18017, 2018.

[10] Y. Li, L. Ji, R. Liu et al., "A review on morphology engineering for highly efficient and stable hybrid perovskite solar cells," *Journal of Materials Chemistry A*, vol. 6, no. 27, pp. 12842–12875, 2018.

[11] Y. Cheng, H.-W. Li, J. Zhang et al., "Spectroscopic study on the impact of methylammonium iodide loading time on the electronic properties in perovskite thin films," *Journal of Materials Chemistry A*, vol. 4, no. 2, pp. 561–567, 2016.

[12] D. Zhao, M. Sexton, H.-Y. Park, G. Baure, J. C. Nino, and F. So, "High-efficiency solution-processed planar perovskite solar cells with a polymer hole transport layer," *Advanced Energy Materials*, vol. 5, no. 6, article 1401855, 2015.

[13] E. H. Jung, N. J. Jeon, E. Y. Park et al., "Efficient, stable and scalable perovskite solar cells using poly(3-hexylthiophene)," *Nature*, vol. 567, no. 7749, article 1036, pp. 511–515, 2019.

[14] Y. Ko, Y. Kim, C. Lee, Y. Kim, and Y. Jun, "Investigation of hole-transporting poly(triarylamine) on aggregation and charge transport for Hysteresisless scalable planar perovskite solar cells," *ACS Applied Materials & Interfaces*, vol. 10, no. 14, pp. 11633–11641, 2018.

[15] M. B. Islam, M. Yanagida, Y. Shirai, Y. Nabetani, and K. Miyano, "NiO_x hole transport layer for perovskite solar cells with improved stability and reproducibility," *ACS Omega*, vol. 2, no. 5, pp. 2291–2299, 2017.

[16] T. Abzieher, S. Moghadamzadeh, F. Schackmar et al., "Electron-beam-evaporated nickel oxide hole transport layers for perovskite-based photovoltaics," *Advanced Energy Materials*, vol. 9, no. 12, article 1802995, 2019.

[17] J. You, L. Meng, T. B. Song et al., "Improved air stability of perovskite solar cells via solution-processed metal oxide transport layers," *Nature Nanotechnology*, vol. 11, no. 1, pp. 75–81, 2016.

[18] J. He, E. Bi, W. Tang et al., "Ligand-free, highly dispersed NiO_x nanocrystal for efficient, stable, low-temperature processable perovskite solar cells," *Solar RRL*, vol. 2, no. 4, article 1800004, 2018.

[19] M. Li, X. Xu, Y. Xie et al., "Improving the conductivity of sol–gel derived NiO_x with a mixed oxide composite to realize over 80% fill factor in inverted planar perovskite solar cells," *Journal of Materials Chemistry A*, vol. 7, no. 16, pp. 9578–9586, 2019.

[20] Y. Cheng, M. Li, X. Liu et al., "Impact of surface dipole in NiO_x on the crystallization and photovoltaic performance of organometal halide perovskite solar cells," *Nano Energy*, vol. 61, pp. 496–504, 2019.

[21] R. Kaneko, H. Kanda, K. Sugawa, J. Otsuki, A. Islam, and M. K. Nazeeruddin, "Perovskite solar cells using surface-modified NiOx nanoparticles as hole transport materials in n-i-p configuration," *Solar RRL*, vol. 3, no. 9, article 1900172, 2019.

[22] J. R. Manders, S.-W. Tsang, M. J. Hartel et al., "Solution-processed nickel oxide hole transport layers in high efficiency polymer photovoltaic cells," *Advanced Functional Materials*, vol. 23, no. 23, pp. 2993–3001, 2013.

[23] M. Li, Y.-M. Xie, X. Xu et al., "Comparison of processing windows and electronic properties between $CH_3NH_3PbI_3$ perovskite fabricated by one-step and two-step solution processes," *Organic Electronics*, vol. 63, pp. 159–165, 2018.

[24] J. Kim, A. Ho-Baillie, and S. Huang, "Review of novel passivation techniques for efficient and stable perovskite solar cells," *Solar RRL*, vol. 3, no. 4, article 1800302, 2019.

[25] Y. Cheng, H.-W. Li, J. Qing et al., "The detrimental effect of excess mobile ions in planar $CH_3NH_3PbI_3$ perovskite solar cells," *Journal of Materials Chemistry A*, vol. 4, no. 33, pp. 12748–12755, 2016.

[26] S. Sajid, A. M. Elseman, H. Huang et al., "Breakthroughs in NiO_x-HTMs towards stable, low-cost and efficient perovskite solar cells," *Nano Energy*, vol. 51, pp. 408–424, 2018.

[27] J. He, Y. Xiang, F. Zhang et al., "Improvement of red light harvesting ability and open circuit voltage of Cu:NiO_x based p-i-n planar perovskite solar cells boosted by cysteine enhanced interface contact," *Nano Energy*, vol. 45, pp. 471–479, 2018.

[28] Y. Nishihara, M. Chikamatsu, S. Kazaoui, T. Miyadera, and Y. Yoshida, "Influence of O_2 plasma treatment on NiO_x layer in perovskite solar cells," *Japanese Journal of Applied Physics*, vol. 57, no. 4S, article 04FS07, 2018.

[29] T. Wang, D. Ding, H. Zheng et al., "Efficient inverted planar perovskite solar cells using ultraviolet/ozone-treated NiO_x as the hole transport layer," *Solar RRL*, vol. 3, no. 6, article 1900045, 2019.

[30] I. Zimmermann, P. Gratia, D. Martineau et al., "Improved efficiency and reduced hysteresis in ultra-stable fully printable mesoscopic perovskite solar cells through incorporation of CuSCN into the perovskite layer," *Journal of Materials Chemistry A*, vol. 7, no. 14, pp. 8073–8077, 2019.

[31] J. Jiang, Q. Wang, Z. Jin et al., "Polymer doping for high-efficiency perovskite solar cells with improved moisture stability," *Advanced Energy Materials*, vol. 8, no. 3, article 1701757, 2018.